5th Intercontinental Geoinformation Days

igd.mersin.edu.tr

Classification of Jilin-1 GP01 hyperspectral image using machine learning techniques with explainable artificial intelligence

Elif Ozlem Yilmaz[*1], **Taskin Kavzoglu** [1]

[1]*Gebze Technical University, Faculty of Engineering, Department of Geomatics Engineering, Kocaeli, Türkiye*

Keywords
Machine learning
Hyperspectral image
Explainable AI
Image classification
Jilin-1 GP01

Abstract

Machine learning (ML) techniques have been significant potential for the image classification; however, they behave as a black box because of the use of unknown descriptors in model construction. Thus, explainable Artificial Intelligence can assist with comprehending the prediction process of a model. In this study, XgBoost and Random Forest were utilized to generate LULC maps for the Özbağ district of Krışehir, a highly forested through the valley, using Jilin-1 GP01 hyperspectral image. Accordingly, the overall accuracies of thematic maps produced by XgBoost and Random Forest were estimated as 93.17% and 91.98%, respectively. Moreover, the Shapley additive explanations (SHAP) technique is employed to understand the output of the models. After SHAP analysis of the ML models, the feature importance of each spectral band was determined. Therefore, given the trained by both algorithms, Band 7 was determined the most important of the hyperspectral bands used in this study. According to the Shapley values, band 5 in the Xgboost model and Band 7 in the random forest model are efficient in class-based evaluations for identifying the bare soil class with the highest F-score value. Although the differences were obtained in the SHAP analysis according to some spectral bands since the working principles of the classification algorithms are different.

1. *Introduction*

Hyperspectral imaging technology has expanded, thanks to its extensive variety of applications and specialties. It provides digital images composed of tens/hundreds of spectral bands which has a tiny range (Kavzoglu and Yilmaz 2022). With the ability to recognize short spectral ranges, hyperspectral images have commonly used widespread applications in numerous fields (Moharram and Sundaram 2022). Particularly, HSI has been utilized extensively in agricultural environmental studies (i.e., land use land cover (LULC) mapping), biology and mineral exploration. Each pixel in HSI relies on characteristics from a small area surrounding the pixel, rather than attributes directly associated with the pixel itself (Liu et al. 2019).

Many techniques used in the early stages of HSI analysis research focused on using the spectral signatures of hyperspectral images for classification. For this purpose, many pixel-wise classification techniques (e.g., Support Vector Machine, Maximum Likelihood, Decision Tree, Random Forest, and eXtreme Gradient Boosting-XgBoost) have been employed for the classification of HSIs (Sothe et al.2020). Furthermore, these techniques have demonstrated outstanding success in the classification of hyperspectral images according to the recent studies (Gore et al. 2021; Moharram and Sundaram 2022) .

Because of the variability of band spectrum, hyperspectral image classification has been recognized in the literature as a complex issue. Consequently, machine learning (ML) approaches have been developed as a useful method for analyzing hyperspectral images. However, ML approaches operate as black boxes despite their considerable capacity in this area (Arrieta et al. 2020).

Artificial intelligence (AI), including machine learning (ML) techniques, can be employed to construct powerful models that provide remarkable prediction or classification performance in a massive variety of difficult areas. Nevertheless, they often have a complex system (i.e., black-box structure), which may impair to ability to comprehend the data. At this point, ML models with explainable AI approaches can be rendered more transparent and interpretable, and consequently their inferences can be helped generate to improve model performance (Arrieta et al. 2020). For instance, SHAP (SHapley Additive exPlanations) algorithm is a commonly employed approach for interpreting black box models (Kavzoglu et al. 2021).

* **Corresponding Author**

*(eoyilmaz@gtu.edu.tr) ORCID ID 0000-0002-6853-2148
(kavzoglu@gtu.edu.tr) ORCID ID 0000-0002-9779-3443

Cite this study

Yilmaz EO & Kavzoglu T (2022). Classification of Jilin-1 GP01 hyperspectral image using machine learning techniques with explainable artificial intelligence. 5th Intercontinental Geoinformation Days (IGD), 145-148, Netra, India

The aim of this work is to evaluate the performance of XgBoost, and Random Forest classifiers using Jilin-1 GP01 hyperspectral image. Besides, this study demonstrates how to interpret the predictions of the aforementioned classification models using an explainable AI method, namely SHAP.

2. Methodology

2.1. XgBoost Algorithm

XgBoost is a gradient-boosted decision tree method, which consecutive decision trees are generated(Chen and Guestrin 2016). The weights are significant parameters because they play a crucial role in this algorithm. In other words, all independent variables that are supplied into the decision tree that used predict outcomes are allocated weights. The weight of variables for which the tree produced incorrect predictions is enhanced, and these variables are then supplied to a second decision tree. Thus, the ensemble of these independent classifiers yields a robust and more accurate model.

2.2. Random Forest Algorithm

Random Forest has become a popular ensemble learning technique for developing predict rules based on multiple types of characteristics without initial assumptions about the relationship amongst dependent features. The success of the algorithm depends on how the decision trees are generated. This technique includes two main steps. In the first step, each tree is created using random samples. Also, whole trees are the same size although being trained in different ways. Two-thirds of the training data is used to train the trees and one-third to evaluate the model. It maintains tree strength while reducing correlation. The second stage uses predictor variables to separate all tree nodes. It is crucial to select few features with enough predictive capacity and minimal correlation (Breiman 2001).

2.3. Interpretation of ML Model

The complex structure of ML algorithms (i.e., XgBoost and Random Forest) makes them difficult to explain and evaluate their outcomes. Explaining model outputs helps to identify the features that affect the model, providing more reliable and robust prediction performance. For this aim, SHapley Additive exPlanations (SHAP) method was utilized to explain and interpret ML model outputs (Lundberg and Lee 2017). It is one of the approaches used for explainable artificial intelligence and is based on the game-theory explaining the performance of a machine learning model. It utilizes the strategy of additive feature importance, which the output of model is stated as the linear addition of parameters of the model input to construct an interpretable method (Kavzoglu et al. 2021).

Tree SHAP is a quick and accurate method for computing SHAP values for tree-based approach including ensemble methods, considering a variety of possible feature dependence assumptions. In this manner, two tree-based ML algorithms (i.e., XGboost and Random Forest) were employed for HSI classification in this study. In addition, Tree SHAP was implemented for explaining the model predictions considering the tree-based architecture of these algorithms.

3. Study Area and Dataset

The Özbağ district of Kırsehir province in Turkey was chosen as the study area (Fig.1.). The Jilin1-GP01 hyperspectral image of June 30, 2021, was used to produce a thematic map of the study area that is a highly forested through the valley.

Figure 1. The study area of Kırsehir in Turkey.

Jilin1-GP01, launched in 2019, is a satellite system with a 12-bit radiometric resolution capable of hyperspectral sensing. The image has three spatial resolutions (5m, 10m and 20m) and consist of a total of 20 spectral bands, including one panchromatic band (Table 1.).

Table 1. Technical specifications of the hyperspectral Jilin1-GP01 satellite image.

Band No	Spectral Range (nm)	Spatial Reso. (m)	Band No	Spectral Range (nm)	Spatial Reso. (m)
B_0	450-800	>5	B_10	698.75-718.75	10
B_01	403-423	5	B_11	732.5-747.5	10
B_02	433-453	5	B_12	773-793	10
B_03	450-515	5	B_13	855-875	20
B_04	525-600	5	B_14	660-670	20
B_05	630-680	5	B_15	677.5-685	20
B_06	784.5-899.5	5	B_16	750-757.5	20
B_07	485-495	10	B_17	758.75-762.5	20
B_08	615-625	10	B_18	935-955	20
B_09	650-680	10	B_19	1000-1040	20

It should be stated that all bands of Jilin-1 GP01 image atmosphericaly and geometrically corrected before image processing stage. The Gram-Schmidt pan-sharpening technique was used to resample 10- and 20-m spatial resolution bands to a 5 m resolution.

According to characteristics of study area, five LULC classes, including impervious surface, soil bare, rock, forest, and vegetation, were used in the classification process to generate thematic maps. In order to implement supervised classifications, the ground-reference dataset was splitted into training and testing

samples. To be more specific, 500 pixels from each LULC class were collected for the training stage while 300 pixels were gathered for the testing stage. Furthermore, the classification application was executed employing Jupyter Notebook with the Python programming language.

4. Results

In this study, pixel-based XgBoost and Random Forest classifiers were used to produce thematic maps. The thematic maps produced with XgBoost and Random Forest classification algorithms are shown in Figure 2.

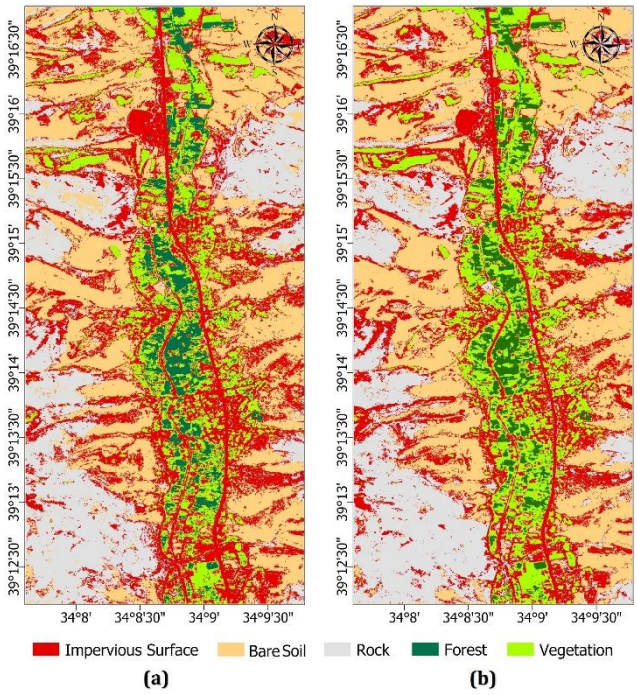

Figure 2. Thematic maps generated with XgBoost classifier (a) and Random Forest classifier (b)

At the end of the classification stage, confusion matrices were estimated (Tab. 3). It should be noted that, equal number of pixels (300 pixels) per LULC class were used in generation of confusion matrices to avoid bias between classes.

The overall accuracies and Kappa coefficients were estimated to analyze the accuracy of the thematic maps. In accordance with this purpose, the overall accuracies of thematic maps produced by XgBoost and Random Forest were estimated as 93.17% and 91.98%, respectively. In addition, the Kappa coefficients were determined as 0.91 and 0.90 for both classifiers (Tab. 3). Besides, F-score values were generated to assess the predicted accuracy of LULC class-specific. The highest F-score values (97.10% with XgBoost classifier and 96.20% with Random Forest classifier) were computed for the bare soil class in two thematic maps, according to Table 3. On the other hand, lowest F-Score values (87.60% with XgBoost classifier and 85.90% with Random Forest classifier) for both thematic maps were calculated for vegetation class. The confusion matrix indicates that the vegetation class is particularly mixtured with the forest class. The primary reason of this situation could be related to spectrally similar characteristics of vegetation and forest class.

Table 3. Predictive performances of XgBoost and Random Forest methods

LULC Class	XgBoost (%)	Random Forest (%)
Impervious Surface	93.30	91.25
Bare Soil	97.10	96.20
Rock	95.55	93.00
Forest	92.30	92.30
Vegetation	87.60	85.90
Overall Acc. (%)	93.17	91.98
Kappa Coef.	0.91	0.90

Combining local interpretations from the SHAP tree explanation function, the SHAP graph scored the most significant spectral bands by importance. In other words, The SHAP method forecasts the estimated marginal contribution of each characteristic. According to Figures 3 and 4, the y-axis shows spectral bands in the hyperspectral dataset, the x-axis depicts the estimated Shapley value, and the color (i.e., blue, purple, pink, orange and green) shows how much of an effect the spectral bands have on the LULC classes.

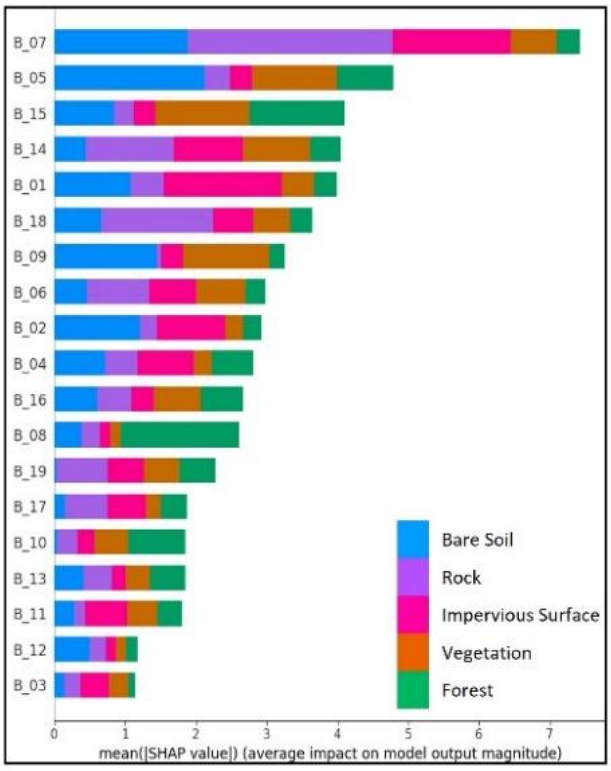

Figure 3. SHAP chart illustrating the feature importances for XgBoost model

The effet of Band 7 of Jilin-1 GP01 image exhibited a more considerable effect on the model output than the other spectral bands, demonstrating that changes to this band can have a significant effect on the outcomes for both ML classifier (Fig. 3). Besides, Band 7 contributes more to the bare soil, rock, and impervious surface classes than the others. On the other hand, it can be said that the first 3 spectral bands affecting the model in the SHAP analysis are located in the visible region. In the

trained Xgboost model, the effect of Band 5 and Band 7 on identifying the bare soil and rock class, respectively, was found to be remarkably considerable.

When Figures 3 and 4 are compared, there are several similarities; yet there are also a few differences. In the SHAP graph for Random Forest, the feature importance of the first four spectral bands is close (Fig. 4.). Furthermore, as in the other SHAP graph for XgBoost classifier, it is observed that the bare soil class is highly affected by Band 7(Fig. 4.). The difference between the SHAP graphs can be attributed to that XgBoot and Random Forest classifier algorithms work with different principles during hyperspectral classification.

When both graphs were analyzed, the common bands with low significance were identified as 11, 12 and 13 Band. It was observed that the study area contains bare soil and rock classes and infrared bands affect the classifier less in the detection of them.

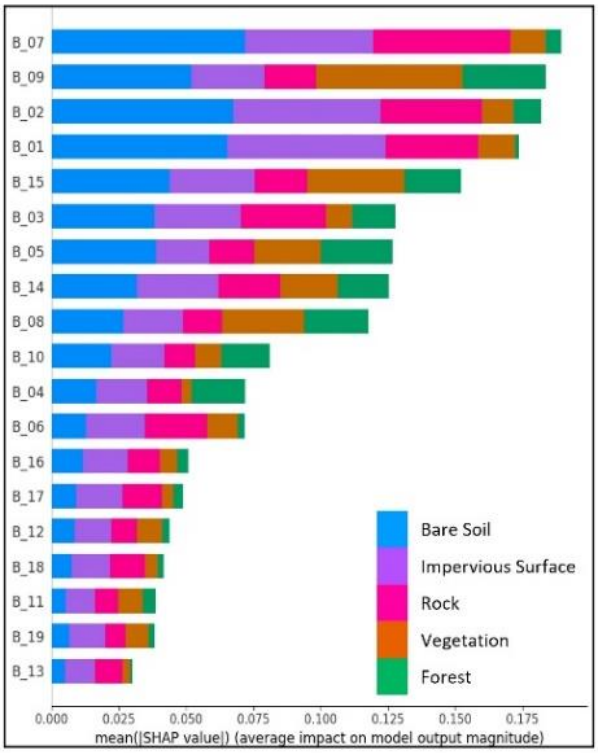

Figure 4. SHAP chart illustrating the feature importance for Random Forest model

5. Conclusion

ML approaches which have been commonly implemented in remote sensing applications were used to create LULC maps in this study. In detailed, it can be said that the performance of XgBoost classifier increased overall accuracy by aprroximately 1%, compared to performance of Random Forest classifier. On the other hand, to examine the performance of the ML algorithms in detail, that is to say, to understand the actions taken by the model and the non-linear relations that exist inside the model, explainable AI approaches are required. Therefore, the SHAP technique was used to interpret the classifier outputs and analyze the importance of spectral bands. Hereby, predicated on the trained by both algorithms, Band 7 was considered the most significant among the other spectral bands utilized in this study. Consequently, SHAP allows in-depth analysis of hyperspectral data and can guide in selecting the appropriate spectral bands and AI model for LULC classification.

References

Arrieta A. B., Díaz-Rodríguez, N., Ser, J. D., Bennetot, A., Tabik, A., Barbado, A., Garcia, S., Gil-Lopez, S., Molina, D., Benjamins, R., Chatila, R., & Herrera, F. (2020). Explainable Artificial Intelligence (XAI): Concepts, taxonomies, opportunities and challenges toward responsible AI, Information Fusion, 58, 82-115.https://doi.org/10.1016/j.inffus.2019.12.012.

Breiman, L. (2001) Random Forests. Machine Learning, 45, 5–32. https://doi.org/10.1023/A:1010933404324

Chen, T., & Guestrin, C. (2016) Xgboost: A scalable tree boosting system. In Proceedings of the 22nd ACM SIGKDD International Conference on Knowledge Discovery and Data Mining, 785-794. https://doi.org/10.1145/2939672.2939785

Gore, R. W., Mishra, A. D., Deshmukh, R. R. (2021). Hyperspectral Image Classification using Machine Learning, 261, 265. https://doi.org/10.1145/3484824.3484883

Kavzoglu, T., Teke, A., & Yilmaz ,E. O. (2021). Shared block-based ensemble deep learning for shallow lanslide susceptibility mapping. Remote Sensing, 13(25), 4776. https://doi.org/10.3390/rs13234776

Kavzoglu, T. & Yilmaz E., O. (2022). Analysis of patch and sample size effects for 2D-3D CNN models using multiplatform dataset: hyperspectral image classification of ROSIS and Jilin-1 GP01 imagery. Turkish Journal of Electrical Engineering and Computer Sciences, 30(6), 2124-2144. https://doi.org/ 10.55730/1300-0632.3929

Liu, S., Marinelli, D., Bruzzone L., & Bovolo, F. (2019). A review of change detection in multitemporal hyperspectral images: Current techniques, applications, and challenges. IEEE Geoscience and Remote Sensing Magazine, 7(2), 140-158. https://doi.org/10.1109/MGRS.2019.2898520.

Lundberg, S. M. & Lee, S. (2017). A unified approach to interpreting model predictions. Advances in Neural Information Processing Systems, 2017,47-4775.

Moharram, M. A. & Sundaram, D. M. (2022). Dimensionality reduction strategies for land use land cover classification based on airborne hyperspectral imagery: a survey. Environmental Science and Pollution Research. https://doi.org/10.1007/s11356-022-24202-2

Sothe, C., De Almeida, C. M., Schimalski, M. B., La Rosa, L. E. C., Castro, J. D. B., Feitosa, R. Q., Dalponte, M., Lima, C. L., Liesenberg, V., Miyoshi G. T., &. Tommaselli A. M. G. (2020) Comparative performance of convolutional neural network weighted and conventional support vector machine and random forest for classifying tree species using hyperspectral and photogrammetric data. GIScience & Remote Sensing, 57(3), 369-394. https://doi.org/10.1080/15481603.2020.1712102